

## Feature Article

# 2019 IEEE Scientific Visualization Contest Winner: Visual Analysis of Structure Formation in Cosmic Evolution

Karsten Schatz , Christoph Müller , Patrick Gralka , Moritz Heinemann , Alexander Straub , Christoph Schulz , Matthias Braun , Tobias Rau , Michael Becher , Steffen Frey , Guido Reina , Michael Sedlmair , Daniel Weiskopf , Thomas Ertl 

Visualization Research Center (VISUS), University of Stuttgart, Germany

Patrick Diehl , Dominic Marcello , Juhan Frank 

Louisiana State University, Baton Rouge, United States

Thomas Müller 

Max Planck Institute for Astronomy, Heidelberg, Germany

**Abstract**—Simulations of cosmic evolution are a means to explain the formation of the universe as we see it today. The resulting data of such simulations comprise numerous physical quantities, which turns their analysis into a complex task. Here, we analyze such high-dimensional and time-varying particle data using various visualization techniques from the fields of particle visualization, flow visualization, volume visualization, and information visualization. Our approach employs specialized filters to extract and highlight the development of so-called *active galactic nuclei* and *filament structures* formed by the particles. Additionally, we calculate *X-ray emission* of the evolving structures in a pre-processing step to complement visual analysis. Our approach is integrated into a single visual analytics framework to allow for analysis of star formation at interactive frame rates. Finally, we lay out the methodological aspects of our work that led to success at the 2019 IEEE SciVis Contest.

■ **COSMIC EVOLUTION**, namely the formation of galaxies and larger structures in the universe, has been a field of study for decades. While observations of distant galaxies and galaxy clusters provide snapshots of the universe at early times, it is impossible to directly observe how a given region

of the universe evolves over billions of years. To study this evolution, cosmological simulations are performed, in which numerous physical quantities are followed in time and analyzed. This in turn requires the development of suitable analysis tools. Therefore, the *SciVis Contest 2019* was dedicated

## Feature Article

to the visual analysis of a cosmological simulation that models the evolution of the universe from the age of five million years ( $z = 200$ ) up to now ( $z = 0$ ), where  $z$  is the redshift. The simulation, conducted using the *Hardware/Hybrid Accelerated Cosmology Code (HACC)* [5] comprises  $64^3$  dark matter particles and  $64^3$  baryon particles contained in a cubic domain with a side length of  $64 Mpc/h$ , where  $h$  reflects the uncertainty of the Hubble constant. For further details about the *SciVis Contest*, please refer to [Background 1](#), for further details on the particle types see [Background 2](#). The task of the contest was to summarize the provided data set. Moreover, studying the impact of active galactic nuclei (AGNs, see [Background 3](#)) on their surroundings is in line with the general goal of the HACC simulation.

Our presented approach to the analysis of the simulation data adopts a variety of different techniques from all areas of visualization. Parallel coordinates plots (PCPs) and scatter plot matrices (SPLOMs) are used to provide an overview of the quantities and to discover patterns in multi-dimensional data. Additionally, these techniques facilitate selection and filtering, using brushing and linking. Further, particles are rendered as spheres, mapping different quantities to size and color, arrow glyphs are used to visualize the velocity of the particles, and direct volume and iso-surface renderings of reconstructed particle densities are employed. As the majority of matter in the universe resides in cosmological filaments and many interesting processes, such as star formation, occur within the filaments or in their vicinity [1], a filament detection algorithm that can separate these structures from the surrounding medium was developed. For the velocities, surface line integral convolution (LIC) is used, which allows to encode the direction of the particles on the surface of dense areas, i.e., on filament structures. Furthermore, a scalar field approximating the X-ray emission in space and time was computed, which is a physical process that can be observed in the universe. All these techniques are combined in a visual analytics tool based on MegaMol [3], which facilitates high-performance rendering for interacting with large simulation data. This allows researchers to explore, summarize, and quantify the structure formation in cosmic evolution.

As this work is an extended version of our

### Background 1: The *SciVis Contest 2019*

The *SciVis Contest* is an annual competition co-located with the IEEE VIS Conference as an associated event. Since 2004, the contest provides scientific data sets for visualization and data analysis by individuals and teams, stoking a competitive spirit in the visualization community. The competitive entries are judged and ranked by domain scientists and visualization experts.

The data set for the 2019 contest originates from a cosmological simulation containing dark matter and baryonic particles. Such simulations pose an opportunity for visualization researchers to apply their techniques and deliver visually stunning and informative imagery to provide domain specialists with a deeper understanding of their data. The participants have been rewarded for techniques exposing science and skill in developing summary information of the data set, creating an animation showing the evolution of the simulation, and showcasing used visualization techniques.

The data set was generated using the *Hardware/Hybrid Accelerated Cosmology Code (HACC)*, that incorporates support for baryonic matter and a mechanism for designating particles as active galactic nuclei (AGN). These simulations aim at studying the impact of feedback from AGNs on the surrounding distribution of matter. AGNs are associated with violent bursts of energy that result from matter accretion onto supermassive black holes at the center of galaxies.

original contest entry [7], the presentation of the used methods will be followed by a discussion of our methodology. Compared to other academic works, the contest setting provides a special environment, which sometimes requires different approaches.

## DATA OVERVIEW

We first want to report on the different steps of the analysis process for the simulation data using our system. In this section, we start with

## Background 2: Baryons and Dark Matter

Baryons are the collective term for elementary particles that make up almost all of the mass of the matter we encounter daily. Well-known examples of baryons are protons and neutrons that build atomic nuclei and, together with electrons, form all of the normal matter around us. Most of the light emitted by stars and galaxies, including active galactic nuclei (AGNs), originates from electromagnetic interactions between baryons and electrons. In contrast, dark matter does not emit light—hence the name—and is composed of some, as yet unknown, non-baryonic massive particles. While dark matter interacts with normal matter through gravity, there is no electromagnetic interaction. Thus dark matter is not revealed directly, but through its gravitational effects on normal matter, for example, the rotation of galaxies and their motion in galaxy clusters.

an overview of the data. The subsequent sections describe various details of the analysis, as well as adapted or novel techniques.

Initially, we inspected the first and last simulation step by depicting particles as solid glyphs. However, this approach was not viable since particles are evenly distributed initially, and throughout the simulation high particle densities lead to significant occlusion. We decided to incorporate a SPLOM and a PCP to account for the multivariate nature of the data set and quickly filter basic quantities in the simulation data.

The first time step is shown in [Figure 1\(a\)](#). Please note the evenly distributed position components, indicating that the particles are initially positioned on a uniform grid (Marker 1). While this circumstance would have also become visible with simple spatial volume rendering, one might have missed the non-evenly distributed high velocities and gravitational potential. Less obvious is the equal distribution of the two classes of particles (all baryon particles have equal mass  $m_b$ , while all dark matter particles have equal  $m_d$ , where  $m_d \approx 5m_b$ ). Presumably, these are the initial values of the simulation.

The last time step is shown in [Figure 1\(b\)](#). Contrary to the beginning of the simulation, one can see the fine filament structures emergent in the position, as well as the normally distributed velocity. As expected, strong correlation between temperature and internal energy can be observed (Marker 2, bottom right scatterplot). Moreover, one can recognize that a large smoothing length correlates with slow particles, which is also backed up by correlation with the gravitational potential (Marker 2, top left scatterplot). Furthermore, entropy is not evenly distributed. The PCP at the top allows for easy detection of correlations between the given magnitudes, as the column order is interchangeable. It also provides brushing and linking based filtering and highlighting of the data as shown in [Figure 1](#).

When inspecting all time steps as an animation (see our video <sup>1</sup>), some leaping values, such as molecular weight and density, can be noticed around time step 35. We account this to the simulation entering the epoch of re-ionization that is commonly modeled by suddenly switching on a ultraviolet background radiation source. Additionally one can observe the overall trend of everything slowing down.

## FILAMENT DETECTION

Especially in later simulation steps of the universe, matter forming filament structures can be observed. Based on previous research [1], those filaments and their surroundings are considered to be of high interest to domain experts as they contain more than half the matter of the known universe. While purely density-based approaches, such as direct iso-surface visualization, usually result in recognizable filament structures, they also tend to cause visual clutter in other regions. Hence, we modified the friends-of-friends algorithm by Davis et al. [2] to isolate the filament structures more reliably, thus facilitating analyses. While this algorithm was originally designed to detect dark matter halos, it suffers from an inherent drawback—the tendency to generate elongated halos. However, in the case of filament structures, which are elongated by nature, this is actually an advantage. Beside the particles, the method requires only one input, the so-called *linking*

<sup>1</sup><https://www.youtube.com/watch?v=ykn3ewqWUcw>

## Feature Article

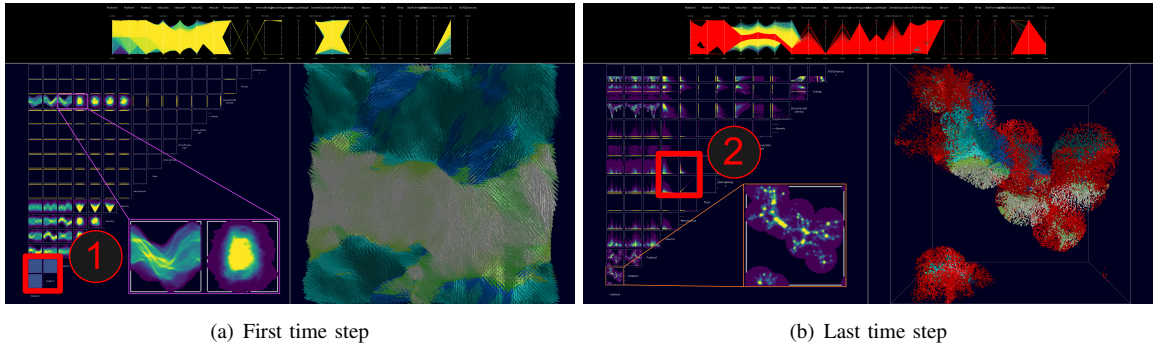


**Figure 1.** Linked visualizations providing an overview of the data. A PCP (top, both figures) and a SPLOM (left, both figures) with high-dimensional points aggregated as density and then mapped to color (kernel density estimation, low-to-high is blue-to-yellow). In addition, position and velocity are encoded into arrow glyphs (right, both figures). Here, the PCP is used to filter for particles close to an AGN and to brush all particles with a low velocity (cf. (b), brushed particles in red). These distance values were not given in the original data and were precomputed by us. Marker 1: Even spatial particle distribution. Marker 2: Correlation between temperature and internal energy, as well as slow particles correlating with a large smoothing length.

### Background 3: Active Galactic Nuclei

An active galactic nucleus (AGN) refers to the bright and compact central region of a galaxy whose electromagnetic luminosity is much higher than usual and cannot be explained by stellar emission. The spectral view of the emission of AGNs typically spans the entire spectrum of electromagnetic radiation, from radio to gamma rays. Commonly, the accepted mechanism for the non-stellar emission is radiation from hot gas falling into a supermassive black hole at the center of a galactic nucleus. Scientists have found supermassive black holes with masses up to billions of solar masses in many galaxies, including our Milky Way.

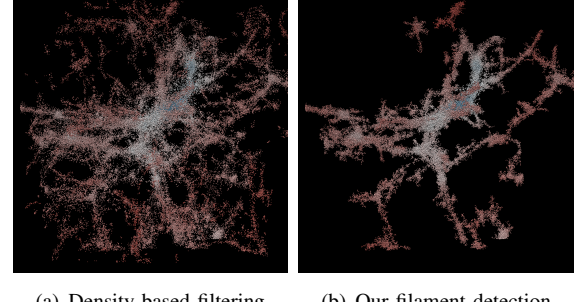


**Figure 2.** Filament detection examples with particles colored by gravitational potential. With the applied settings, smaller filaments are filtered out alongside unrelated particles. It is possible to include the smaller filaments filtered out in (b) by tweaking the parameters of the method, but this would also add some of the clutter that can be seen in (a), which uses a purely density-based filtering of the particles. Width of the shown structure: 64 Mpc/h

length  $l$ . Particles belong to the same cluster if they are closer than said linking length.

Filament structures are typically the densest regions of the data set. Therefore, we adapted the original method to only select clusters that host at least one particle with a density value larger than 90% of the maximum density; all other clusters are filtered out. Subsequently, small-sized clusters with a particle count below a certain threshold (1000 in this case) are also dropped. For the results of the detection method shown in Figure 2, the linking length was set to  $l = 450 \text{ kpc}/h$ .

## FILAMENT PARTICLE FLOW

Showing the particle flow in the vicinity of filaments helps understanding the impact of large-scale gravitational influences on structure formation. To do so, a density representation is computed from the particles by splatting density kernels around the positions of all particles, accumulating at a point in space:

$$\rho(\vec{x}) = \sum_p k(||\vec{x} - \vec{x}_p||, h) \rho_p, \quad (1)$$

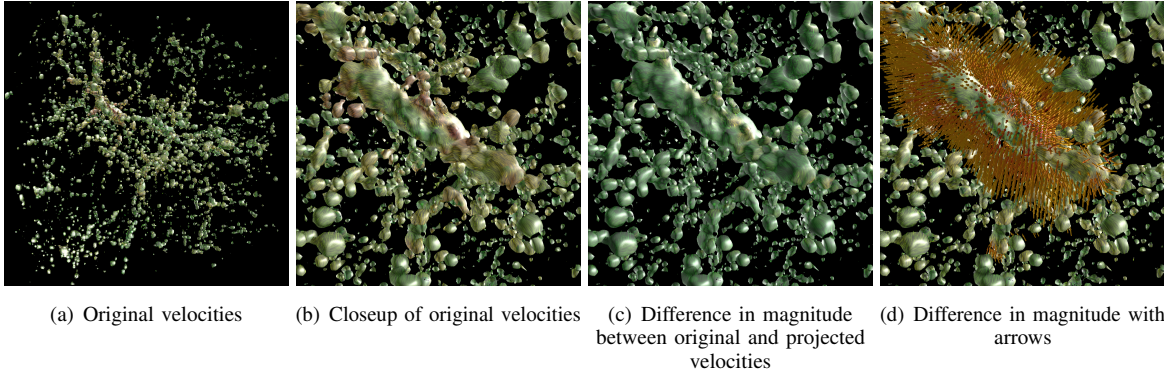


**Figure 3.** Surface LIC rendered on a reconstructed iso-surface. Colors indicate the velocity magnitude, ranging from low (green) to high (red). Original velocities are shown in (a) and (b). Difference between original and projected velocities are shown in (c). Arrow glyphs in (d) point toward dense structures, indicating continued growth as expected. The base of the arrow is located at the corresponding particle position. Shown structure widths are: 64  $\text{Mpc}/\text{h}$  for (a) and 12  $\text{Mpc}/\text{h}$  for (b), (c), and (d).

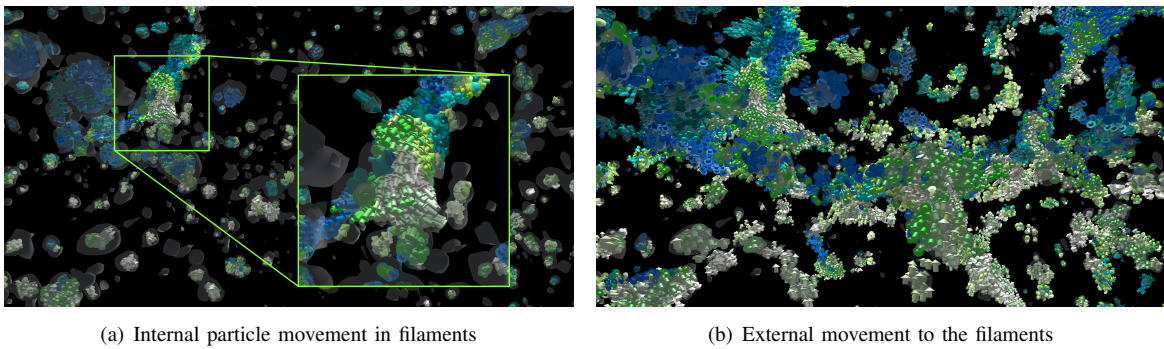


**Figure 4.** Density iso-surfaces depicted alongside with density-filtered velocity arrows for particles (colored by velocity direction). (a) Internal particle movements are revealed by using a higher density threshold. The inset shows how particles flow along the filament structure. (b) Movement of outside particles selected by using a lower density threshold for filtering. As opposed to the internal ones, the outer particles move toward the filament structures. Their movement seems to be coordinated as many particles have a similar velocity direction. Shown structure widths: 32  $\text{Mpc}/\text{h}$  for (a) and (b), and 5  $\text{Mpc}/\text{h}$  for the highlighted structure of (a).

where  $p$  is a particle at position  $\vec{x}_p$ ,  $\rho_p$  is its density value, and  $k$  is a radial basis function with the smoothing length  $h$  as kernel size. From the resulting density volume, an iso-surface encompassing areas of high density can be extracted.

To investigate the movement of particles in the vicinity of such a reconstructed surface, velocity information is interpolated at arbitrary positions, in a manner similar to the density splatting described above. Here, the velocity is interpolated using inverse distance weighting:

$$\vec{u}(\vec{x}) = \frac{\sum_p k(||\vec{x} - \vec{x}_p||, h) \vec{u}_p}{\sum_p k(||\vec{x} - \vec{x}_p||, h)}, \quad (2)$$

with velocity  $\vec{u}_p$  at position  $\vec{x}_p$ .

The resulting 3D vector field can be used

to depict the flow of particles on the extracted surfaces. For this, a hybrid screen-space variant of line integral convolution (LIC) [10] is used. To capture the flow on the surface, the velocity is projected onto the surface, normalized and then used for streamline computation. Convolving the values from a noise texture along the streamline with a symmetric filter kernel yields the LIC texture visualizing the flow direction. Velocity magnitude is then encoded by color. To distinguish between near and far objects, visual highlights using Phong shading for a fixed light source is added. The result is shown in Figure 3. The small differences in magnitudes (c) indicate that the velocities are mostly tangential to the surface.

## Feature Article

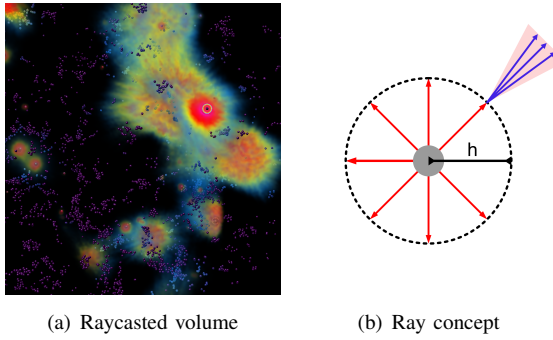


**Figure 5.** (a) Raycasted X-ray emission volume of time step 490 rendered alongside with AGNs and star candidate particles. The highest visible emission is radiated from the only active AGN particle. Shown structure width: 60 Mpc/h. (b) Schematic of ray-generation at a particle for the volume step.

However, additionally showing arrows in the vicinity of the cluster in (d) allows us to infer that the particle flow is directed toward the surface before reaching it. Figure 4 further illustrates this behavior.

### X-RAY EMISSION

The particles in the data set depict matter that emits electromagnetic waves. Some of these particles emit in the X-ray spectrum, which is of particular interest. The reconstruction of the X-ray emission allows us to validate the assumption that AGNs, like other massive stellar objects, should emit X-rays (see [Background 4](#)), as well as to monitor how AGN activity influences the thermal evolution of the vicinity. To show a qualitative illustration of X-ray irradiance in the data set, we implemented a raycasting-based method that generates and renders a volume capturing approximated instantaneous X-ray transport through the volume. The approach is inspired by the visualization model of Magnor et al. [6] and the irradiance volume technique of Greger et al. [4].

In our method, X-ray emission is accumulated for each voxel and attenuated by the absorption, but other effects or functions, such as scattering or radiance distribution functions, are neglected. The overall process comprises two steps, for which the equations given in [Background 4](#) are used. Note that for these computations the image is scaled to a range of [0, 1] per time step.

In the first step, the X-ray emissivity of each

baryon particle is determined using [Equation 3](#). In the second step, rays are shot from each particle position into the volume to capture the emission from the particle attenuated by [Equation 4](#) at each voxel traversed by the ray. To avoid “self-illumination”, the ray origins are offset by the smoothing length, hence sampled uniformly on a sphere around the particle position. Starting at each of the resulting offset positions, multiple rays are spawned, their directions sampled in a cone, whose centerline is defined by the offset vector (see [Figure 5\(b\)](#)).

Note that the quantities in [Equation 3](#) are retrieved for each individual particle. In contrast, the quantities in [Equation 4](#) are splatted into volumes (see [Equation 1](#)) prior to ray traversal in the pre-processing steps.

Once the X-ray emission volume is computed (and the voxel values scaled to a range of [0, 1] per time step), it is rendered using a classic direct volume raycasting approach. As can be seen in [Figure 5](#), this approach highlights possible AGN candidates and AGN particles, which helps guide the user’s attention to these areas, independent of the currently depicted quantities.

### STAR FORMATION

Based on feedback from our domain scientists, we analyzed the formation of stars, which happens in cold areas with high density. [Figure 6](#) shows the top 10 % of the densest particles and the bottom 10 % of the coldest ones.

In an animation of the timeline, one can see star-forming gas being converted to stars. Preceding the classification of the particles as star-forming gas, the molecular weight of the particles increases. However, this is only a necessary, but not a sufficient condition for star formation.

Furthermore, one can observe the formation of AGNs in the vicinity of star clusters when more and more star-forming gas starts to accumulate in those areas. However, the AGN classification is being revoked as the star-forming gas starts to disappear. This behavior is expected since AGNs feed on matter, such as star-forming gas, and suspend their activity without further mass nearby. The presumption is reinforced by the observation that some AGNs keep “waking up” when fueled by new gas. Such behavior is also known as *AGN duty cycle*, as the AGN activity is correlated to

## Background 4: X-rays

X-rays are a form of high-energy electromagnetic radiation with wavelengths shorter (more energetic) than ultraviolet and longer (less energetic) than gamma rays. In most astrophysical situations, X-rays are emitted by highly ionized gas or plasma at temperatures in the range of millions to hundreds of millions of Kelvin [2]. The X-ray emission discussed in this article is caused by very hot low-density gas falling towards the central regions of galaxy clusters, which are dominated gravitationally by massive galaxies.

According to our domain scientists, it is possible to approximate the X-ray emissivity of baryon particles in line with Dolag et al. [1], by approximating emissivity from Bremsstrahlung

$$\epsilon_X \approx \rho^2 \sqrt{T}, \quad (3)$$

where  $\rho$  is the density and  $T$  is the temperature of a particle. After being emitted, the X-rays are partially absorbed by the surrounding medium. In our illustration, the absorption coefficient is

approximated by

$$\alpha \approx 0.018 \sqrt{T^{-3}} 1.4 \left( \frac{\rho}{m} \right)^2 g. \quad (4)$$

[Equation 4](#) is adapted from equation 5.19b from Rybicki and Lightman [3]. Since the data set does not contain information about the number density of electrons or ions, density  $\rho$  and mass  $m$  are used to compute  $1.4 \rho^2/m^2$ , a replacement suggested by our domain scientists for the term  $Z^2 n_e n_i$  in the original equation. Moreover, the frequency was not included in the equation, and the Gaunt factor  $g$  was assumed to be 1.2 (cf. Sect. 5.2 [3]).

## ■ REFERENCES

1. K. Dolag, S. Borgani, S. Schindler, A. Diaferio, and A. M. Bykov. Simulation techniques for cosmological simulations. *Space Sci Rev*, 134(1):229–268, 2008.
2. H. Gursky. The X-ray emission from rich clusters of galaxies. *Publ Astron Soc Pac*, 85:493, 1973.
3. G. B. Rybicki and A. P. Lightman. *Radiative Processes in Astrophysics*. John Wiley & Sons, 2004.

the star-formation rate.

## METHODOLOGY

The Design Study Methodology (DSM) by Sedlmair et al. [8] is an attempt of formalising the process of designing and validating a visualization system for a real-world problem. They propose a process comprising nine stages and identify a total of 32 pitfalls researchers should avoid while conducting a design study. The *SciVis Contest* takes place in a similar setting in that it is a project to design visualizations for a specific problem and validate these against the tasks of the contest. However, some aspects of their work are not applicable to the contest setting and some of the pitfalls are inherent to it.

The *SciVis Contest* clearly conforms to the majority of the characteristics Sedlmair et al. used to define a design study: it is a project (several people working on a specific task for a limited time), it tackles a real-world problem (even if it might be a simplified version like in our case) and

the goal is showcasing visualization as problem solving method in a coherent system. However, the characteristic collaboration with real users and their real data is somewhat limited: while the organizers of the contest are typically available to answer the participants' questions, the process of working on a solution does not involve showing them iterations of the visualizations and asking for feedback. No close collaboration between the visualization experts and the domain experts is possible. In fact, the real user in form of the contest organizers only gets to see the final solution. Therefore, we reached out to colleagues we knew to be experts in parts of the target domain of astrophysics as “proxy” of the real-world user. Albeit such an approach of adding more experts instead of selecting the right one is the exact opposite of the *winnow* phase suggested in the DSM, we reckon having a variety of domain experts at hand gave us access to expertise for large portions of the application field. Given the very open task of 2019’s contest, the experts

## Feature Article

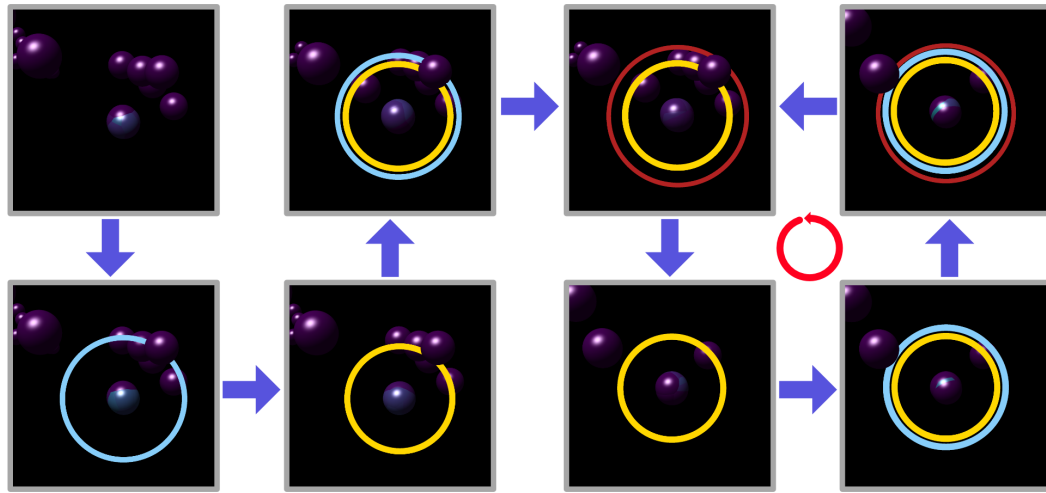


**Figure 6.** Illustration of particles filtered by density and temperature, focusing on one specific AGN. The particles are colored by molecular weight (purple low, blue high). Additionally, circles highlight star-forming gas (blue), stars (yellow), and AGN particles (red). The process of AGN creation is shown in the left four figures. The right four figures visualize the found fuel cycle where the AGN becomes active and inactive again.

provided us with valuable ideas like computing X-ray emissions to relate the simulation data with phenomena measurable in the real universe. Nevertheless, Sedlmair et al.’s PF-7 (researcher expertise does not match domain problem) remains a latent problem as the domain scientists consulted in this way are not the ones having produced the data and did not phrase the underlying research questions. Furthermore, a role allocation, as suggested for the third stage (*cast*), is not really possible, because many aspects that describe a role are dependent on the ownership of the data and the interests regarding their analysis. However, some of the colleagues could be seen as *liaisons* in the sense of the work of Simon et al. [9]. That is, collaborators that are experts in both the visualization and the target domain.

As the task of the contest, and our solution in particular, also required expertise in many different sub-fields of visualization, the first stage of the DSM (*learn*) at first seems to be very time-consuming as the obvious approach to it is few researchers gaining knowledge in all of the sub-fields. We opted for a second approach, incorporating people who already had insight in the literature of their respective field. In some cases, we did this even a fair amount into the later phases of the project as new visualization requirements emerged from discussing intermediate results. Fortunately,

the *SciVis Contest* of 2015 had a similar task and we were able to leverage much of the knowledge gained from the old data. This, of course, does not include in-depth knowledge of the current data itself and, most importantly, of the intents behind the simulation and its real-world goals, so this stage required large amounts of guesswork, from visualization and domain experts alike. To close this knowledge gap, the fourth stage (*discover*) and the following two stages (stage 5: *design*; stage 6: *implement*) were conducted in an iterative, exploratory manner, as more and more details about the data became clear.

Starting from the fifth stage of the DSM, the hard time limit in the contest scenario becomes a critical factor. Several pitfalls mentioned by Sedlmair et al. (PF-24, PF-28, PF-32) relate to time as an issue. Oftentimes, the question for us was not “Is it possible?”, but “Is it possible in the given time frame?” We therefore implemented those ideas that promised to be the most distinctive ones considering the competitive nature of the contest. As the iterative approach to design and implementation required quick iterations, we used our in-house visualization framework MegaMol [3]. The modular structure of the software allowed fast and parallel (among multiple colleagues) prototyping of the considered methods. Furthermore, many colleagues being familiar with

the software helped us bringing their expertise and existing implementations into the project on-demand in the aforementioned way. The final team included specialists for particle visualization, flow visualization, information visualization, and volume visualization. It is worth mentioning that in the end, most of the development work was in the field of data processing rather than visualization, as most of the basic visualization methods were already available through MegaMol. The team therefore could produce an application with decent interactive performance by adapting these methods. Furthermore, the built-in video production facilities of the software is a factor not to be underestimated in context of the *SciVis Contest*.

Sedlmair et al.'s *deploy* phase is not applicable in the contest scenario, because the user in form of the contest organizers does never use the visualization software, but judges the outcomes based on the written submission, the accompanying video and the poster. Typically, the goals of the *write* stage are also different in that the *SciVis Contest* typically poses more or less specific questions about the data that have to be answered in the submission. The way how the visualization software developed helped finding these answers is more of an implicit outcome. In our case, the software as well as the found answers were a collaborative effort from domain and visualization experts alike. While some of the presented methods, such as the X-ray visualization and the display of particle flow inside the filaments, were inspired by the domain scientists, other methods, such as the filament filtering and the surface LIC, were contrived by our visualization experts.

## CONCLUSION

In our work, we presented various visualization techniques, which we combined in a visual analytics system based on the software framework MegaMol. Using SPLOMs and PCPs, correlations between properties, as well as their distributions, can be visualized. Through brushing and linking, particles can be filtered or highlighted. Our adapted filament detection algorithm can be used to focus the analysis on filaments and thereby on the vicinity of AGNs. Visualizing flow on the filament surfaces, we gained insight into

the movement of particles close to the centers of galaxies. X-ray emission additionally helps in identifying AGNs and visualizing their potential. Finally, the type of particles can be depicted using circles, which we used to identify and analyze the fueling process of AGNs.

Afterwards, we reflected on the process of developing the visualizations for the very open task of the *SciVis Contest 2019*. In this part, we compared how this scenario connects to the Design Study Methodology of Sedlmair et al. and where the contest setting deviates from the more standard visualization research behind this methodology.

In the future we would like to apply our visualization framework to larger cosmological data sets. In current works some data sets comprise  $1000^3$  particles instead of the  $64^3$  depicted here. Obviously, for such data sets some parts of the visualization pipeline will be better suited than others. Applying out-of-core techniques, the three-dimensional particle visualization methods should scale easily to larger data sets. The interactivity of the SPLOM and the PCP, on the other hand, could suffer from using larger data. This comes from the fact that these methods do not render each particle once but multiple times and could be alleviated by strongly filtering the data for interesting parts before using these methods. The two preprocessing techniques, namely filament detection and X-ray volume generation would be further slowed down by large data. While the filament detection should scale quite reasonably with larger data sizes due to its used acceleration structures, the current version of the X-ray calculation might take days or even weeks, depending on the actual size. After the preprocessing is finished, the rendering of the results could work at an interactive frame rates, as the size of the output volume is independent from the data set size. Therefore, the scaling of the X-ray precomputation will be an interesting problem to research in the future.

## ACKNOWLEDGMENTS

This work was partially funded by DTIC Contract FA8075-14-D-0002/0007 and the Center of Computation & Technology at Louisiana State University; by Deutsche Forschungsgemeinschaft (DFG) as part of the Cluster of Excellence EXC 2075 “SimTech” (390740016), Transregional Collaborative Re-

## Feature Article

search Centres SFB/Transregio 75 (84292822) and SFB/Transregio 161 (251654672), Collaborative Research Centre SFB 1244 (279064222), the International Research Training Group GRK 2160 “DROPIT” (270852890), and “Research Software Sustainability for the Open-Source Particle Visualization Framework MegaMol” (391302154); by the German Bundesministerium für Bildung und Forschung (BMBF) as part of project “TaLPas” (Task-based Load Balancing and Auto-tuning in Particle Simulations); by Baden-Württemberg Stiftung as part of project “DiHu” (High Performance Computing II grant); and by Intel Corporation as part of the Intel Graphics and Visualization Institutes of XeLLENCE program. Additionally, we want to thank JD Emberson and the HACC team at Argonne National Laboratory for making their data available for the *IEEE SciVis Contest 2019*.

## ■ REFERENCES

1. P. A. R. Ade, N. Aghanim, M. Arnaud, M. A. J. Ashdown, F. Atrio-Barandela, J. Aumont, C. Baccigalupi, A. Balbi, A. J. Banday, R. B. Barreiro, et al. Planck intermediate results - VIII. Filaments between interacting clusters. *Astron Astrophys*, 550:A134, 2013.
2. M. Davis, G. Efstathiou, C. S. Frenk, and S. D. M. White. The evolution of large-scale structure in a universe dominated by cold dark matter. *Astrophys J*, 292:371–394, 1985.
3. P. Gralka, M. Becher, M. Braun, F. Friess, C. Müller, T. Rau, K. Schatz, C. Schulz, M. Krone, G. Reina, and T. Ertl. MegaMol - A comprehensive prototyping framework for visualizations. *Eur Phys J Spec Top*, 227(14):1817–1829, 2019.
4. G. Greger, P. Shirley, P. M. Hubbard, and D. P. Greenberg. The irradiance volume. *IEEE Comput Graph Appl*, 18(2):32–43, 1998.
5. S. Habib, A. Pope, H. Finkel, N. Frontiere, K. Heitmann, D. Daniel, P. Fasel, V. Morozov, G. Zagaris, T. Peterka, et al. HACC: Simulating sky surveys on state-of-the-art supercomputing architectures. *New Astron*, 42:49–65, 2016.
6. M. A. Magnor, K. Hildebrand, A. Lintu, and A. J. Hanson. Reflection nebula visualization. In *IEEE Visualization*, pages 255–262, 2005.
7. K. Schatz, C. Müller, P. Gralka, M. Heinemann, A. Straub, C. Schulz, M. Braun, T. Rau, M. Becher, P. Diehl, D. Marcello, J. Frank, T. Müller, S. Frey, G. Reina, D. Weiskopf, and T. Ertl. Visual analysis of structure formation in cosmic evolution. In *IEEE Scientific Visualization Conference (SciVis)*, pages 33–41, 2019.
8. M. Sedlmair, M. Meyer, and T. Munzner. Design study methodology: reflections from the trenches and the stacks. *IEEE Trans Vis Comput Graph*, 18(12):2431–2440, 2012.
9. S. Simon, S. Mittelstädt, D. A. Keim, and M. Sedlmair. Bridging the gap of domain and visualization experts with a liaison. In *Eurographics Conference on Visualization (EuroVis) - Short Papers*, pages 127–131, 2015.
10. D. Weiskopf and T. Ertl. A hybrid physical/device-space approach for spatio-temporally coherent interactive texture advection on curved surfaces. In *Proceedings of the Graphics Interface Conference*, pages 263–270, 2004.

## Visualization Research Center (VISUS)

University of Stuttgart, Germany

{firstname}.{lastname}@visus.uni-stuttgart.de

**Karsten Schatz** is a doctoral researcher, focusing on the visualization of protein-solvent systems and cosmological simulations.

**Christoph Müller** is a doctoral researcher, whose research interests include graphics clusters, large high-resolution displays and security visualization.

**Patrick Gralka** is a doctoral researcher, interested in visualization of large particle-based data, and parallel methods for GPUs and HPC environments.

**Moritz Heinemann** is a doctoral researcher, focusing on the visualization of multiphase flow.

**Alexander Straub** is a doctoral researcher, whose research interests lie in the field of multiphase flow visualization.

**Christoph Schulz** is a doctoral researcher, focusing on quantification and visualization of uncertainty.

**Matthias Braun** is a research software engineer, whose field of work includes research data management and development of sustainable research software.

**Tobias Rau** is a doctoral researcher, interested in visualization of large-scale physiology simulations on HPC systems and CPU rendering techniques.

**Michael Becher** is a doctoral researcher, focusing on visual computing for structural engineering.

**Steffen Frey** is a research associate, whose work is focused on performance-related aspects and expressive visual representations of dynamic processes.

**Guido Reina** is a research associate, his research interests including visualization of large data and

parallel methods, and visualization software design.

**Michael Sedlmair** is a junior professor, with interests on information visualization, interactive machine learning, virtual and augmented reality, and evaluation methodologies underlying them.

**Daniel Weiskopf** is a professor, whose research interests include information visualization and scientific visualization, visual analytics, eye tracking, computer graphics, and special and general relativity.

**Thomas Ertl** is a professor, his research interests including visualization, computer graphics and human-computer interaction.

### **Center of Computation & Technology**

Louisiana State University, United States

*pdiehl@cct.lsu.edu | dmarrce504@gmail.com*

**Patrick Diehl** is a research scientist, focusing on computational mathematics, high performance computing, and scientific visualization.

**Dominic Marcello** is a research scientist, whose field of work includes computational astrophysics and high performance computing.

### **Department of Physics and Astronomy**

Louisiana State University, United States

*frank@phys.lsu.edu*

**Juhan Frank** is a professor, his current research interests including mass transfer in close binary stars and stellar mergers.

### **Max Planck Institute for Astronomy**

Heidelberg, Germany

*tmueller@mpia.de*

**Thomas Müller** is a research associate, whose area of interest includes the visualization of astronomical and astrophysical phenomena.